Ibn Al-Haitham Journal for Pure and Applied Sciences
Journal homepage: jih.uobaghdad.edu.iq
PISSN: 1609-4042, EISSN: 2521-3407
IHJPAS. 2025, 38 (1)

New Boric Acid Derivative with Some of Its Complexes and Study the Biological and Anticancer Activity

Alaa Abdullah Majeed[1*] and Asmaa Mohammed Noori[2]
[1,2] Department of Chemistry, College of Sciences, University of Baghdad, Baghdad, Iraq
*Corresponding Author.

Received: 16 April 2023 Accepted: 23 July 2023 Published:20 January 2025
doi.org/ 10.30526/38.1.3418

Abstract

Background Spectral methods such as Fourier transform infrared spectroscopy, ultraviolet-visible spectroscopy, and proton nuclear magnetic resonance (^{1}H-NMR) spectra, along with thermal analysis (TG/DTA), elemental analysis (CHN), and melting point, were used to characterize the synthesized compounds. This study conducted additional examinations for metal complexes, including molar conductivity, magnetic susceptibility, chloride, and metal content. Objectives This study aims to synthesize and characterize a novel ligand and its metal complexes with cobalt, nickel, and platinum complexes and to evaluate their potential biological activities through focusing on their antibacterial, antifungal and anticancer properties. Materials and Methods A new ligand (5-(2-benzamido-N-methylacetamido)-4-((3,4,5-trimethoxycyclohexa-1,3-dien-1-yl) methyl) pyrimidine-2-yl)amino)boric acid was synthesized by the reaction of trimethoprim amide derivative with boric acid, as well as its metal complexes with cobalt, nickel, and platinum. Results All synthesized complexes have octahedral geometry; cobalt and nickel complexes are nonelectrolytes, while platinum complexes are electrolytic. This study tested all the synthesized compounds as antibacterial and antifungal agents against *Staphylococcus aureus*, *Pseudomonas aeruginosa*, and *Candida albican*. Additionally, this study tested the new ligand and its platinum complexes as anticancer agents against adenocarcinoma human cells (A549). Conclusion Thus study have achieved positive outcomes for every complex's antibacterial, antifungal, and anticancer properties.

Keywords: Trimethoprim, boric acid, cobalt complex, nickel complex, platinum complex.

1. Introduction

Producing novel compounds with antimicrobial and anticancer activities uses trimethoprim, a crucial synthetic ligand material (1). Trimethoprim is an antibiotic combined with sulfonamide, a standard treatment for various bacterial infections. It works by inhibiting the production of folic

acid, which is essential for bacterial growth. Boric acid, on the other hand, is an inorganic compound with antifungal and antiseptic properties (2). X-ray crystallography prepared and identified a trimethoprim-boric acid compound (3). Researchers have carried out investigations into the antimicrobial and anticancer properties of trimethoprim-boric acid. Researchers have also found the compound to have potent anti-proliferative activity against various cancer cells, including those of the breast, lung, and colon (4). Various studies (5, 6) have demonstrated borate's anticancer and antibacterial benefits with ligands and metal trimethoprim. The studies reported that to fight the growing threat of widespread antibiotic resistance, there is a need for innovative antimicrobial medications (7,8). Furthermore, recent studies have shown platinum complexes also have anticancer solid properties, which are cytotoxic to various cell types (9, 10). The current research synthesized a new boric acid derivative ligand from a trimethoprim amide derivative to enhance its medicinal and biological properties. This study also makes metal complexes of this amide ligand with cobalt (II), nickel (II), and platinum (IV) [Co (II), Ni (II), and Pt (IV), respectively] metal ions to make it more biologically active. A physicochemical and spectral inspection of all produced compounds has been conducted to support the proposed structures. This study evaluated the biological and anticancer activity of the synthetic compound.
This study aims to synthesize and characterize a novel ligand, 5(2-benzamido-N-methylacetamido)-4-((3,4,5-trimethoxycyclohexa-1,3-dien-1yl) methyl) pyrimidine-2-yl) amino) boric acid, and its metal complexes with Co (II), Ni (II), and Pt (IV) also to investigate the biological activity of the ligand and its complexes.

2. Materials and Methods

2.1. Synthesis of ((5-(2-benzamido-*N*-methylacetamido)-4-((3,4,5-trimethoxy-cyclohexa-1,3-dien-1-yl) methyl) pyrimidin-2-yl) amino) boric acid

The ligand **Figure 1** was synthesized by adding boric acid (0.1 g, 1.6 mmol) to a warm solution of N-(2-((2-amino-4-((3,4,5-trimethoxycyclohexa-1,3-dien-1-yl) methyl) pyrimidine-5-yl) (methyl)amino)-2-oxoethyl) benzamide (previous work) (11). In 6 mL H_2O, a mixture was heated under reflux with stirring for 15 hours (the reaction was terminated after TLC tested the solution). The off-white powder was obtained after cooling the solution in an ice bath; it was washed with ice water and dried in the oven at 80 ºC (12,13).

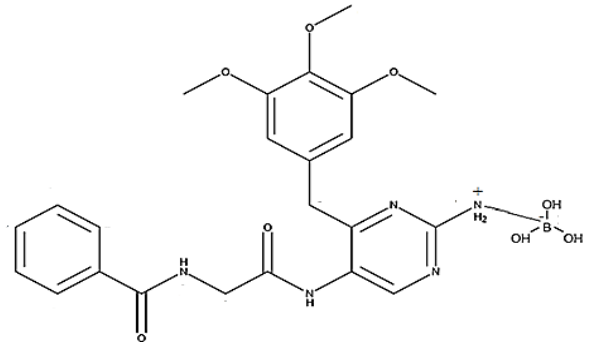

Figure 1. The suggested structure of the prepared ligand.

2.2. Synthesis of Co (II) , Ni (II) and Pt (IV) complexes (C1,C2 and C3)

The mixture of ligand (0.1 g, 0.194 mmol) in 6 mL water and metal salts (2:1, L: M) in 4 mL water (**Table 1)** was heated under reflux for 5 hrs. with stirring. Heating evaporates a portion of the solvent. The product was collected by crushing it in an ice bath, washing it with ice water, and drying it in an oven at 80 ºC. **Figures 2- 4** display the suggested structures of the complexes.

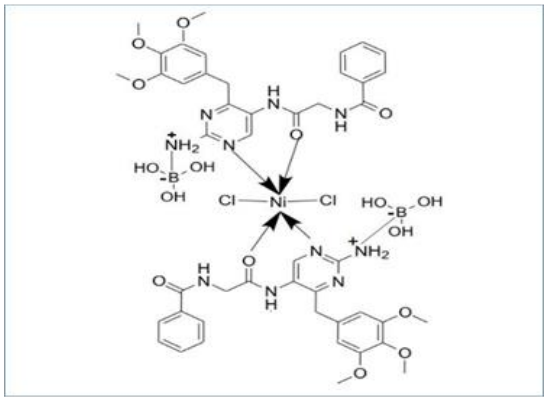

Figure 2. The structure of Ni(II) complex.

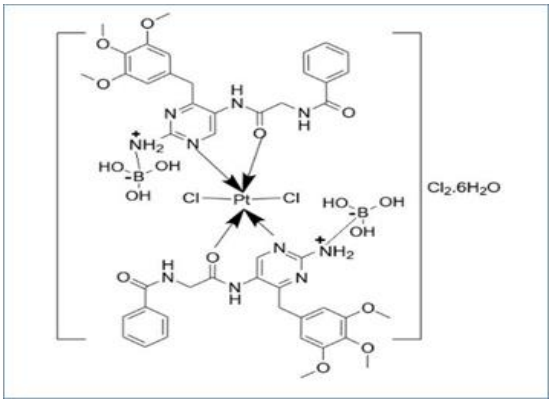

Figure 3. The structure of Pt(IV) complex.

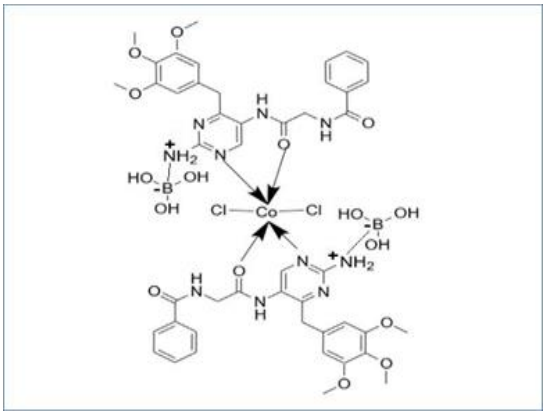

Figure 4. The structure of CO(II) complex.

Table 1. The optimization conditions for synthesis of complexes.

No	Ligand (wt(g),mmol) in 6 mL H_2O	Metal salts (wt(g),mmol) in 4 mL H_2O	Color of precipitate	Color of solution
C_1 Co(II)	L (0.1 g,0.194 mmol)	[$CoCl_2.6H_2O$] (0.023g ,0.097 mmol)	Pale blue	Reddish pink
C_2 Ni(II)	L (0.1 g,0.194 mmol)	[$NiCl_2.6H_2O$] (0.023g,0.097 mmole)	Light green	Green
C_3 Pt(IV)	L (0.1 g,0.194 mmol)	[K_2PtCl_6] (0.047g,0.097 mmol)	Brown	Yellow

2.3. Anticancer

For anticancer detection, each of the 96 flat-well microtiter plates held $1x10^4$–$1x10^6$ cells/mL of tumor cell culture media. The microplate was wrapped with Parafilm to prevent contamination and gently shaken before use. After removing the incubation media and incubating the plates at

37 ºC with 5% carbon dioxide for 72 hours, two-fold dilutions of the target chemical (50, 100, 200, and 400 mg/mL) were added to the wells. Tests were performed in triplicate at each concentration and with the controls (cells treated with serum-free medium). The plates were exposed for the appropriate amounts of time.

2.4. Antimicrobial Activities

All synthesized compounds have been evaluated for antibacterial action against *Pseudomonas aeruginosa, Staphylococcus aureus,* and *Candida albicans* when tested at 10^{-2} M in DMSO solutions using the agar diffusion method. Inhibition radii were used to determine their efficacy against bacteria and fungi (14).

3. Results and Discussion

3.1. Physical properties and elemental microanalysis

Tables 2 and **3** contain information on the metal concentration (atomic absorption), (C.H.N.), physical characteristics, and the name of the ligand and its metal complexes. Based on (C.H.N.), atomic absorption analysis, chloride content, spectral data, magnetic measurement, and thermal analysis, the molecular formulas of the investigated compounds were proposed.

Table 2. Elemental analysis and physicochemical characteristics of ligand and metal complexes.

Comp.	The molecular formulae	Color	m.p (°C)	Yield %	M.wt g.mol^{-1}	Elemental Micro Analysis (Found) Calc.			Metal content %	Chloride content %
						C%	H%	N%		
L	$C_{23}H_{28}N_5O_8B$	Off white	194-196	84-90	513.282	56.87 (56.02)	6.14 (5.64)	15.62 (14.89)	_	_
C_1Co(II)	$[C_{46}H_{56}N_{10}O_{16}B_2Co.Cl_2]$	Pale blue	184-188	83-87	1156.494	50.24 (49.53)	5.27 (4.84)	15.22 (14.08)	5.09 (5.4)	6.13 (6.5)
C_2Ni(II)	$[C_{46}H_{56}N_{10}O_{16}B_2Ni.Cl_2]$	Light green	188-190	86-91	1156.254	50.90 (50.14)	5.34 (4.84)	14.81 (14.08)	5.07 (4.1)	6.14 (5.74)
C_3Pt(IV)	$[C_{46}H_{56}N_{10}O_{16}B_2Pt.Cl2]$ $6H_2O.2Cl$	Brown	228-230	90-94	1471.654	36.38 (37.25)	3.91 (4.42)	11.72 (11.01)	_	9.64 (8.5)

Table 3. ligand and its metal ion complex by their respective names and formulas.

Comp.	The molecular formula	Name
L2	$C_{23}H_{28}N_5O_8B$	((5-(2-benzamido-*N*-methylacetamido)-4-((3,4,5-trimethoxycyclohexa1,3-dien-1-yl)methyl)pyrimidin-2-yl)amino)boric acid
C_1 Co(II)	$[C_{46}H_{56}N_{10}O_{16}B_2Co.Cl2]$	DiChloro[bis((5-(2-benzamido-*N*-methylacetamido)-4-((3,4,5-trimethoxycyclohexa-1,3-dien-1-yl)methyl)pyrimidin-2-yl)amino)boric acid cobalt(II)]
C_2 Ni(II)	$[C_{46}H_{56}N_{10}O_{16}B_2Ni.Cl2]$	DiChloro[bis((5-(2-benzamido-*N*-methylacetamido)-4-((3,4,5-trimethoxycyclohexa-1,3-dien-1-yl)methyl)pyrimidin-2-yl)amino)boric acid Nickle(II)]
C_3 Pt(IV)	$[C_{46}H_{56}N_{10}O_{16}B_2Pt.$ $Cl2].6H_2O$ .2Cl	Di chloro [bis ((5-(2-benzamido-*N*-methylacetamido)-4-((3,4,5-trimethoxycyclohexa-1,3-dien-1-yl)methyl)pyrimidin-2-yl)amino)boric acid platinum(IV)] chloride hexa hydrate.

3.2. The FT-IR spectroscopy

It has been revealed that the FTIR spectra of Co, Ni, and Pt complexes changed in the way the ω (C=O) amide and ω (C=N) groups stretched, which was caused by the ligand interacting with metal ions through the ω (C=O) amide and ω (C=N) group (15,16). **Figures 5-8** display the ligand and complex spectra. The spectra of the ligand and its complexes showed the appearance of a new band at 1338 cm^{-1} due to the υ (B-O) and 1375 cm^{-1} due to the υ (B-N) (17). A new band appeared at low frequency, which was attributed to (υ M-N), (υ M-O), and (υ M-Cl) (18). There is no change in O-H and NH_2 stretching vibrations, as shown in **Table 4**.

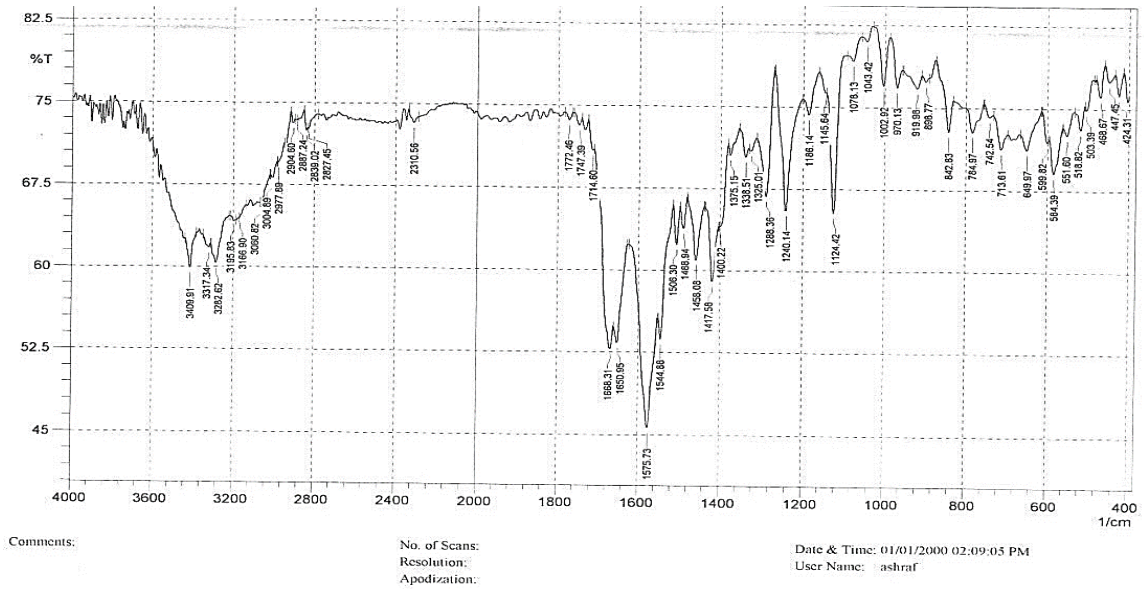

Figure 5. Fourier transform infrared spectrum of the ligand.

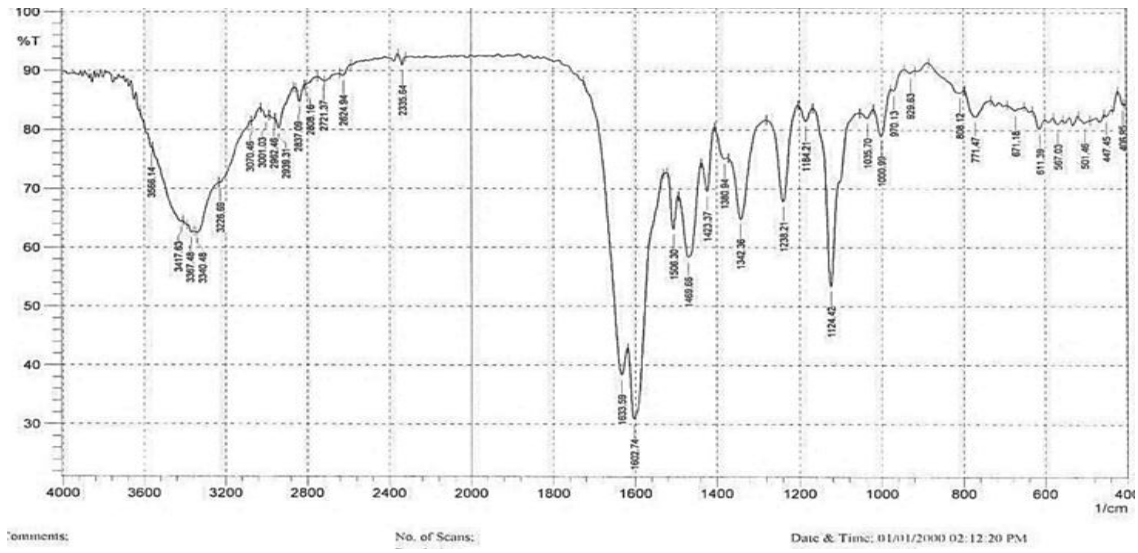

Figure 6. Fourier transform infrared spectrum of a platinum complex.

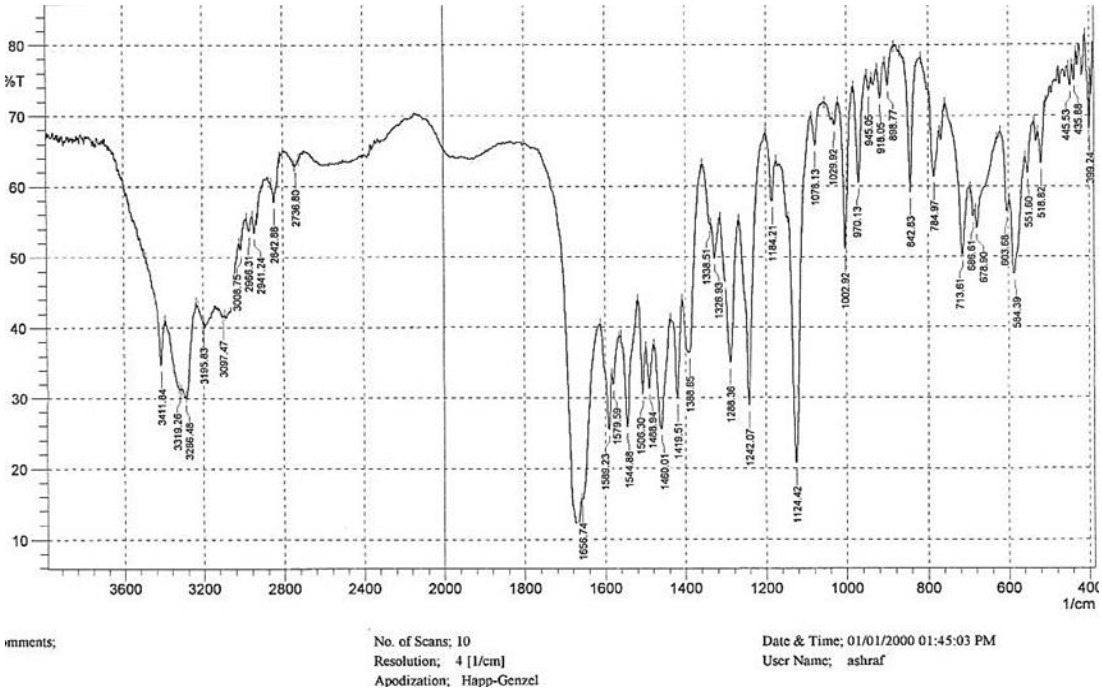

Figure 7. Fourier transform infrared spectrum of a nickel complex.

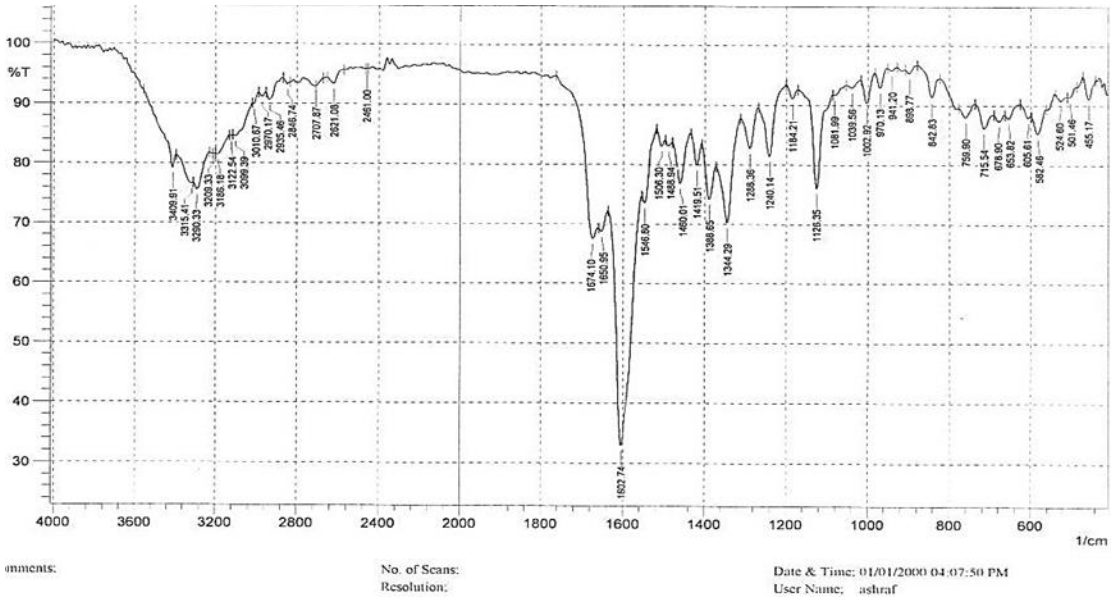

Figure 8. Fourier transform infrared spectrum of a cobalt complex.

Table 4. The FT-IR data of ligand and it complexes.

No	Comp	O-H	υ NH_2	υ N-H amide	υ C=O amide	C=N	B-O	υ B-N	M-O	υM-N	υM-Cl
1	**L**	3409	3282asy 3195sy	3317	1668	1575	1338	1375	_	_	_
2	C_1 Co(II)	3409	3290asy 3209sy	3315	1674	1602	1344	1388	582	455	343
3	C_2 Ni(II)	3411	3286asy 3195sy	3319	1656	1589	1338	1388	520	445	337
4	C_3 Pt(IV)	3417	3226asy 3070sy	3317	1633	1602	1342	1380	576	447	343

3.3. The ^{1}HNMR spectra

The ligand (L) was characterized using ^{1}H-NMR in d6-DMSO, as shown in **Figure 10**. In the ligand's ^{1}H-NMR spectrum, there was a singlet peak at ε (2.5) ppm, which was caused by the chemical shift of the solvent d6-DMSO. The other peak at ε (3.2) ppm was caused by H_2O protons in DMSO as impurities (19). Ligand's spectra revealed a new peak at approximately 8.64 ppm, attributed to B-OH (20), with additional peaks in **Table 5**, **Figure 9** depicts the ligand's structure.

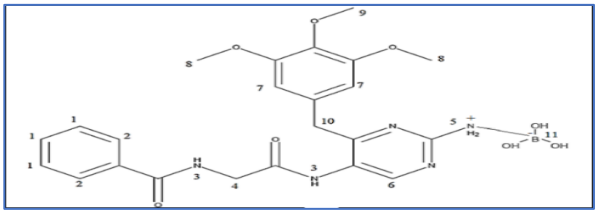

Figure 9. Structure of the ligand.

Table 5. The ^{1}H-NMR data of the ligand.

Assignments in d^6 -DMSO	Mark	Chemical shifts δ (ppm)
Methylene protons	10	(3.58), 2H ,s
Methyl protons	9	(3.64), 3H ,s
Methyl protons	8	(3.87), 6H ,s
Aromatic protons	7	(6.61), 2H ,d
Amine protons	5	(7.08), 2H ,m
Piperazinyl protons	6	(7.48), H ,m
Aromatic protons	1, 2	(7.55)3H, d
BOH protons	11	8.64, 3H ,s
Amide protons	3	(8.92), 2H ,d

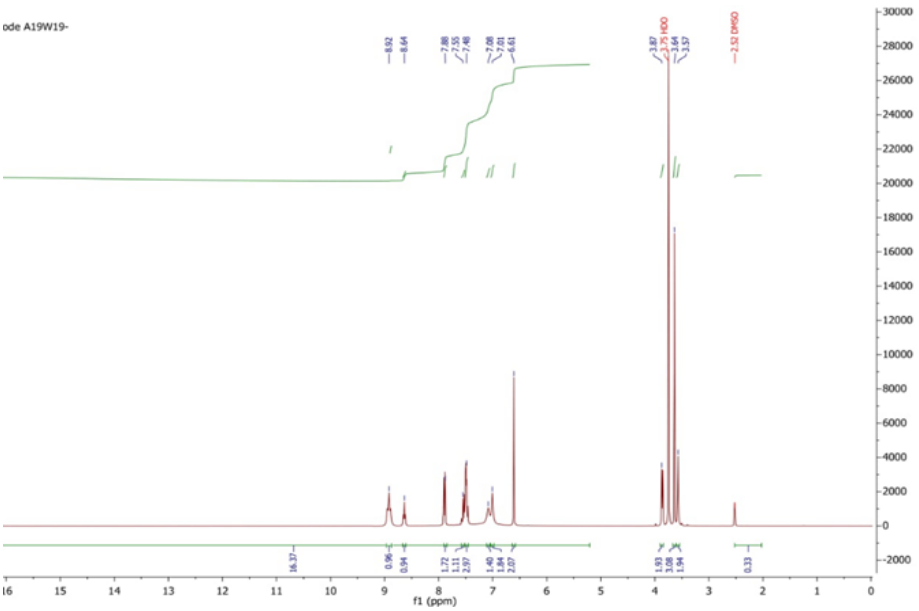

Figure 10. The ^{1}HNMR spectrum of the ligand.

3.4. Thermal analysis of the ligand and its metal complexes

Thermogravimetric (TG) and DTA were measured in argon gas at 25 to 800 °C (10 °C/min). **Table 6** contains thermal dissociation data; **Figures 11–14** display thermographs of ligands and their metal complexes.

Table 6. Thermal decomposition data of the ligand and its complexes.

Comp.	Molecular formula and molecular weight g/mole	Steps	Temp. rang of the decomposition °C	Suggested formula of loss	Mass loss% Cal. (Found)	DTA °C
L2	$C_{23}H_{28}N_5O_8B$	1	0-33	CH_3	1.881(2.928)	_
		2	33-162	$O+2(OCH_3)+OH$	17.74(18.521)	115 (EXO)
	513.282	3	162-300	$B(OH)_2+NH_2+C_6H_2+CH_2+C_4N_2H+NH$	47.07(46.957)	210 (EXO)
		4	300-581	$C_6H_5+CO+H_2$	21.85(20.870)	435 (EXO)
		residue	581-800	NH+C+CO	11.64(10.722)	575 (EXO)
C_1 Co (II)	$[C_{46}H_{56}N_{10}O_{16}B_2Co.Cl_2]$	1	0–38	$2CL+6(OCH_3)+2OH$	24.84(25.16)	75 (EXO)
		2	38–314	$4(OH)+2B+2NH_2+2C_6H_2+4CH_2+3CO+2NH$	51.07(51.32)	_
	1156.494	3	314–562	$CO+2NH+C4HN_2+C_2H$	13.88(13.083)	375 (EXO)
		residue	562–800	Co+ CN	10.21(9.59)	555 (EXO)
C_2 Ni(II)	$[C_{46}H_{56}N_{10}O_{16}B_2Ni.C_{l2}]$	1	0 – 33	$2CL+4(OCH_3)$	16.19(16.86)	_
		2	33–297	$2(OCH_3)+2(C_6H_2)+4CH_2+2B+6OH+4CO_2NH_2+NH$	62.75(62.06)	_
	1156.254	3	297–619	$2NH+C_3HN$	6.898(7.005)	200 (EXO)
		residue	619-800	$C4HN_2+Ni+CN$	14.16(13.98)	300 (EXO)
[illegible]	$[C_{46}H_{56}N_{10}O_{16}B_2Pt.$	1	0–33	$6(H_2O)+4CL+3(OCH_3)$	22.82(23.31)	_

Comp.	Molecular formula and molecular weight g/mole	Steps	Temp. rang of the decomposition °C	Suggested formula of loss	Mass loss% Cal. (Found)	DTA °C
	2Cl].6H_2O+2Cl	2	33 –362	3(OCH_3)+6OH+2B+2NH_2+ 2C6H_2+2CH_2+C_3H	31.41(31.39)	180 (EXO)
	1471.654	3	362–533	NCN+2(C_6H_5)+2CO+2NH	18.74(19.04)	510 (EXO)
		residue	533-800	2CH_2+2CO+Pt+2NH+N_2HC_4	27.03(26.24)	_

3.5. Electronic spectra

The electronic spectra of synthetic compounds were performed at ambient temperature in methanol (10^{-3}M). **Table 5** is a list of all the information about electronic spectra.

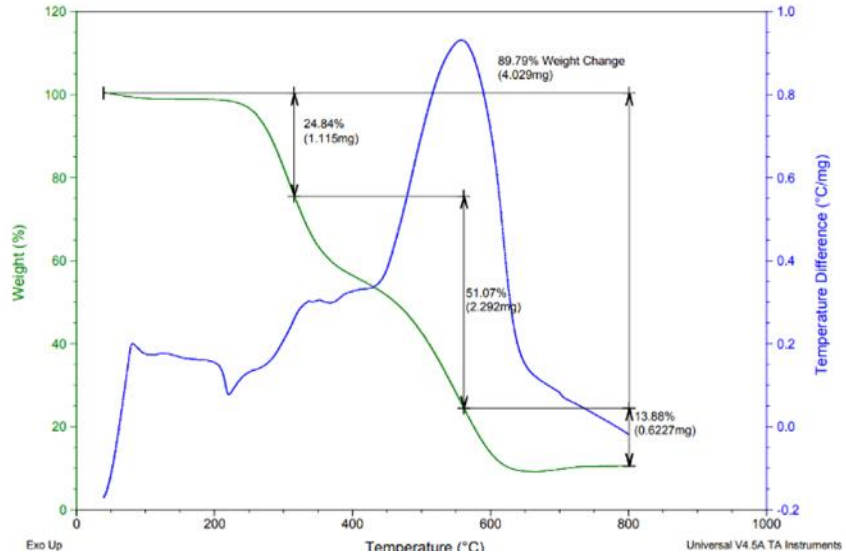

Figure 11. Thermogram of the ligand.

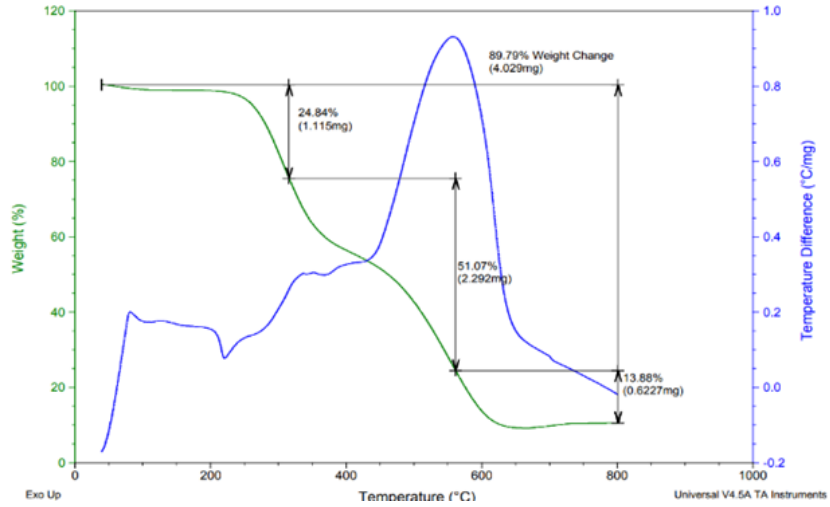

Figure 12. Thermogram of cobalt complex.

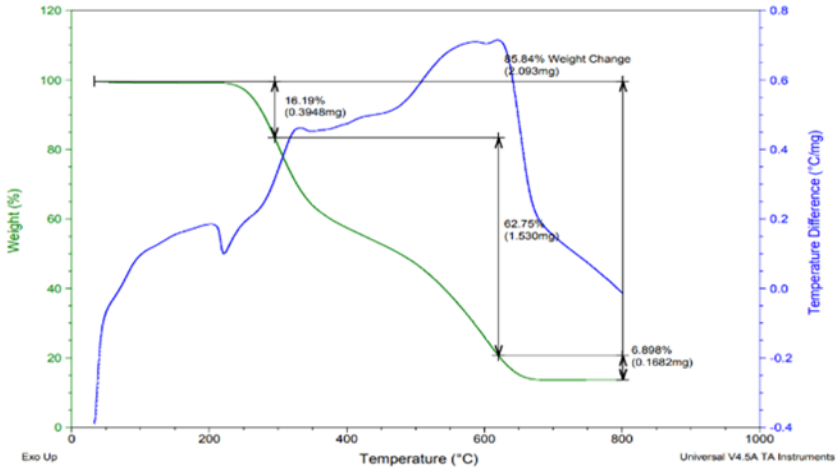

Figure 13. Thermogram of nickel complex.

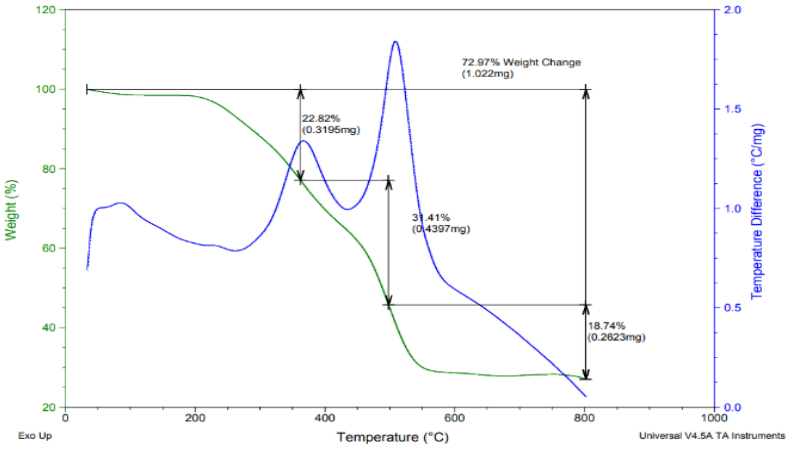

Figure 14. Thermogram of platinum complex**.**

3.5.1. Electronic spectrum of the ligand

The ligand's electronic spectrum showed strong bands at 271 nm (36900 cm^{-1}) and 236 nm (42372 cm^{-1}), caused by the (π -π*) transition (21). The data are shown in **Table 5**, and the ligand's spectrum is shown in **Figure 15**.

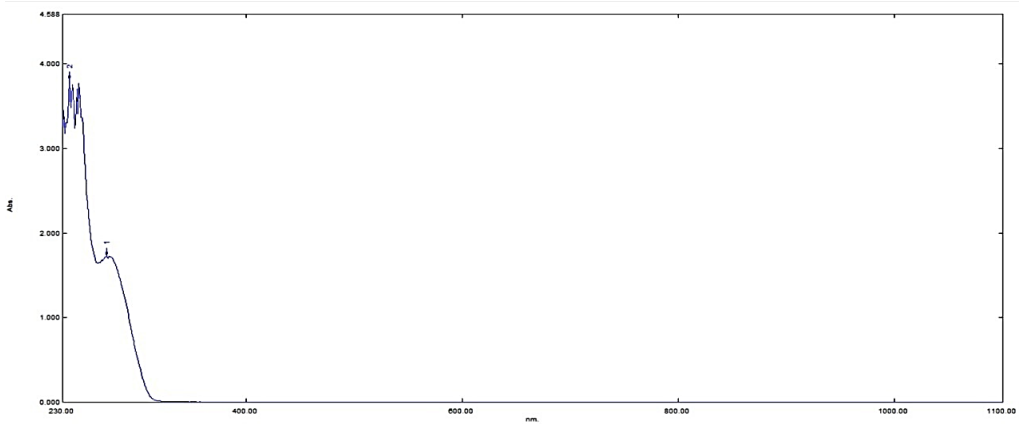

Figure 15. The UV-Vis spectrum of the ligand.

3.5.2. Electronic spectrum of Co (II) complex (C1)

The spectrum of the (C1) in **Figure 16** and the data are listed in Table 5. The Co complex exhibited three bands at 967 nm (10341 cm^{-1}), which refers to $^4T1g \rightarrow {}^4T2g$ transitions, and the other at (861 and 511 nm), (11614 and 19569 cm^{-1}), relates respectively to ($^4T1g \rightarrow {}^4A_2g$ and $^4T_1g \rightarrow {}^4T_1g(P)$) transitions for the octahedral geometry (22,23). The result of conductivity showed that the Co complex was nonelectrolyte and the μeff. The value in **Table 5** is assigned to the Co complex's octahedral geometry (24).

3.5.3. Electronic spectrum of Ni (II) complex (C2)

The spectrum of the (C2) complex is displayed in **Figure 17**, and the data are listed in **Table 5**. The Ni complex indicated two bands at (976 nm) (10245 cm^{-1}); this band refers to $^3A_2g \rightarrow {}^3T_2g$, transition and 540 nm (18518 cm^{-1}), which refers to $^3A_2g \rightarrow {}^3T_1g$ transition for the octahedral geometry (25,26). The conductivity result showed that the Ni complex was nonelectrolyte, and the μ_{eff}—value in **Table 5.** was assigned to the octahedral geometry of the Ni complex (27).

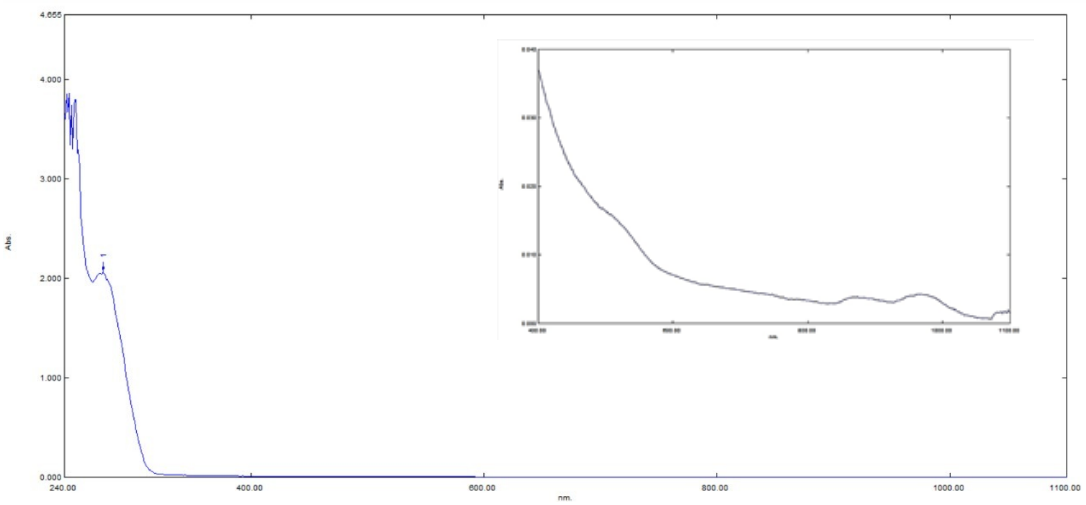

Figure 16. The UV-Vis spectrum of cobalt complex C1.

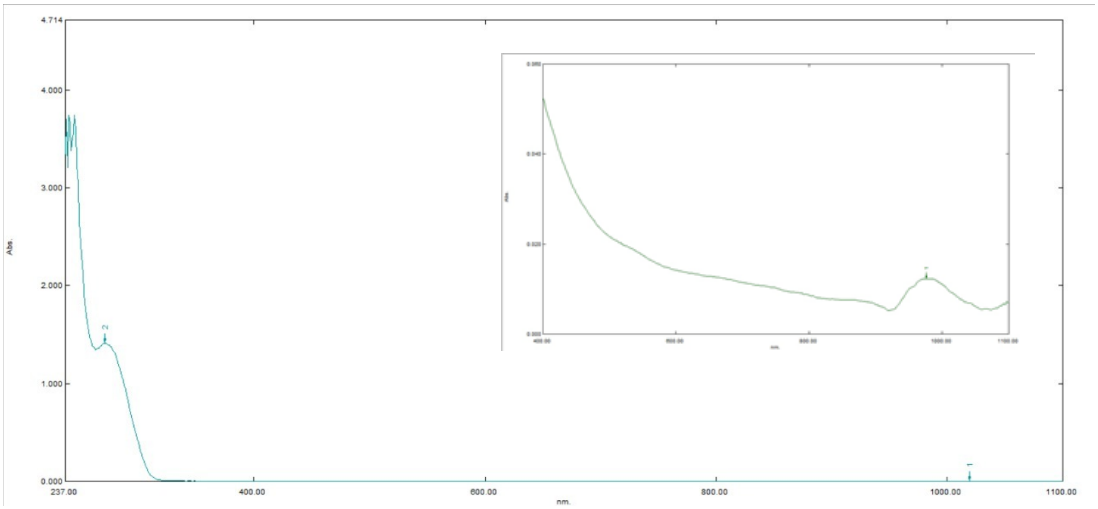

Figure 17. The UV-Vis spectrum of nickel complex C2.

3.5.4. Electronic spectrum of Pt (IV) complex (C3)

The spectrum of the C3 complex is shown in **Figure 18**, and the data are listed in **Table 7**. The Pt complex exhibited two bands at (737 and 914 nm) (13568 and 10940 cm^{-1}), respectively; these bands refer to $^1A_1g \rightarrow {}^3T_1g$ and $^1A_1g \rightarrow {}^3T_1g(H)$ transition (28,29). The result of conductivity showed the electrolytic nature of the Pt complex. The magnetic property of the Pt (IV) complex was diamagnetic (30).

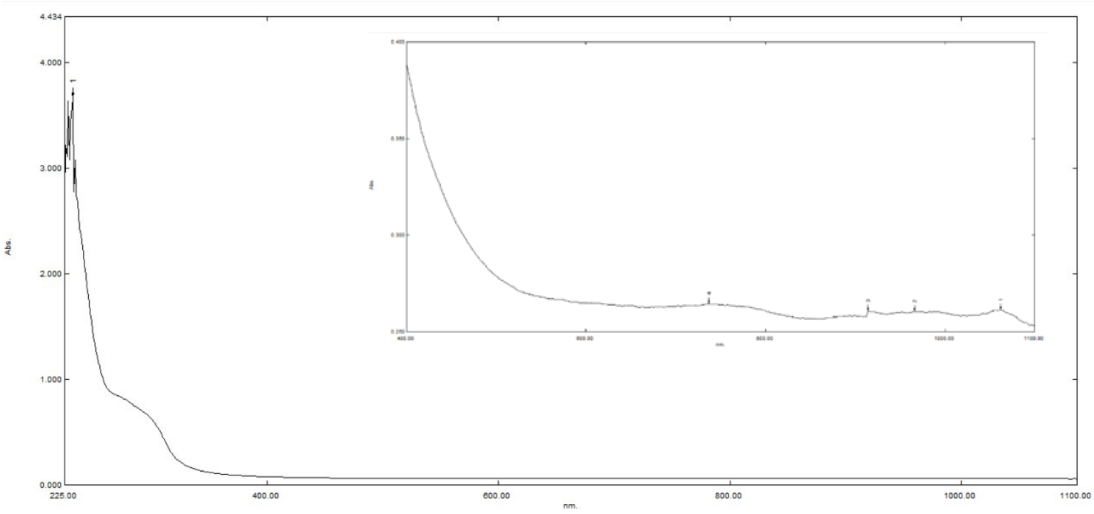

Figure 18. The UV-Vis spectrum of platinum complex C3.

Table 7. Electronic spectra of ligand and complexes.

Comp	Band positions nm (cm^{-1})	Assignment	Molar conductivity ($S.cm^2.mol^{-1}$) in H_2O	$\mu_{eff.}$ (B.M)	Suggested geometry
Ligand	271 (36900)	$\pi \rightarrow \pi^*$		—	—
	236(42372)	$\pi \rightarrow \pi^*$			
C_1	241 (41493)	$\pi \rightarrow \pi^*$	63	5.46	Octahedral
Co(II)	273(36630)	$\pi \rightarrow \pi^*$			
	511(19569)	$^4T_1g \rightarrow {}^4T_2g$ (P)			
	861(11614)	$^4T_1g \rightarrow {}^4A_2g$			
	967 (10341)	$^4T_1g \rightarrow {}^4T_2g$			
C_2	232 (43103)	$\pi \rightarrow \pi^*$	76	3.14	Octahedral
Ni(II)	271(36900)	$\pi \rightarrow \pi^*$			
	540(18518)	$^3A_2\ g \rightarrow {}^3T_1g$			
	976 (10245)	$^3A_2\ g \rightarrow {}^3T_2g$			
C_3	232 (43103)	$\pi \rightarrow \pi^*$	123	Diamagnetic	Octahedral
Pt(IV)	290(34482)	$\pi \rightarrow \pi^*$			
	737 (13568)	$^1A_1\ g \rightarrow {}^3T_1g$			
	914(10940)	$^1A_1\ g \rightarrow {}^3T_1g(H)$			

3.6. Biological activity (Antimicrobial activity)

The antimicrobial properties of the ligand and its metal complexes were conducted utilizing the fusion method at 10^{-2} M in DMSO. All compounds' antibacterial and antifungal activities were tested against (*Pseudomonas aeruginosa, Staph,* and *Candida albicans*). The order of activities for ligand and its complexes was C1(Co) > C2(Ni) > C3(Pt)> L in *Pseudomonas aeruginosa* depending on inhibition zone (18>17>16>14) mm respectively, while in *Staphylococcus aureus* the order was C2Ni > C1(CO) >L > C3(Pt) at inhibition zone (31>30>25>18) mm, respectively.

For *Candida albicans*, the order was C1(Co) > C2(Ni) > C3(Pt) >L at inhibition zone (30>28>27>22) mm, respectively. The ligand and its complexes have more activity than the original compounds (trimethoprim and hippuric acid) against *Candida albicans* and *Staphylococcus aureus*, as shown in **Table 8** and **Figure 19**.

Table 8. The biological activity for studied compounds in (10^{-2} M).

Compounds	*Candida albicans*	*Staphylococcus aureus*	*Pseudomonas aeruginosa*
DMSO	-ve	-ve	-ve
Hippuric	14	15	14
Trimethoprim	13	17	18
L	22	25	14
C1(Co)	30	30	18
C2(Ni)	28	31	17
C3(Pt)	27	18	16

Figure 19. The inhibition zone for ligand and its complex against *Pseudomonas aeruginosa*, *Staph* and *Candida albicans.*

3.7. Anticancer

Adenocarcinoma human cells (A549) were used in a 3-(4,5-dimethylthiazol-2-yl)-2,5-diphenyltetrazolium bromide (MTT) assay to test the cytotoxic effect of the ligand and its complexes. The findings showed that trimethoprim and ligand inhibited the vitality of A549 cells throughout a concentration range of (400-50) g/mL, while the same doses only slightly affected normal cells. The ligand and trimethoprim underwent a 72-hour cytotoxic study. The data shows trimethoprim has a more substantial killing effect than the ligand, as illustrated in **Tables 9, 10** and **Figures 20, 21**.

Table 9. The cytotoxic effects of trimethoprim on the A549 tumor cell line and a normal cell line HDFn.

Cell line	**Conc. µg/mL**				**IC_{50} µg/mL**	**P value**
	400	200	100	50		
A549	32.91	41.09	52.51	62.69	28.91	
	±2.17	±1.34	±3.69	±2.89		<0.0001
HDFn	61.42	72.84	83.99	91.59	208.9	
	±1.69	±2	±1.58	±2.68		

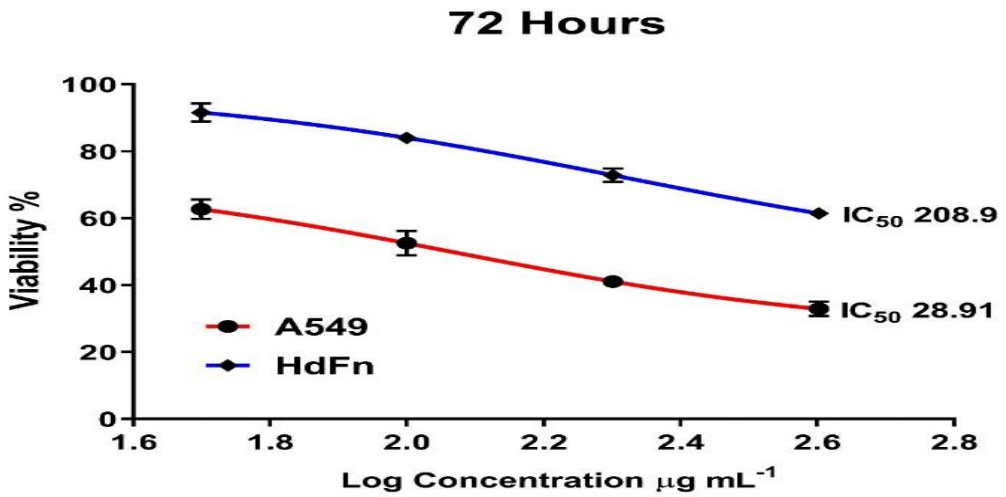

Figure 20. The cytotoxic effect of trimethoprim on A549 cells after 72 hours of incubation at 37 degree Celsius (Log for the original concentration).

Table 10. Cytotoxicity effects of ligand against A549 tumor cell line and normal cell line HDFn.

Cell line	Conc. µg/mL				IC_{50} µg/mL	P value
	400	200	100	50		
A549	63.23 ±2.68	66.98 ±6.09	79.54 ±6.71	95.1 ±0.66	88.44	<0.0001
HDFn	74.31 ±3.73	86.07 ±1.92	95.22 ±0.82	95.95 ±1.03	212.8	

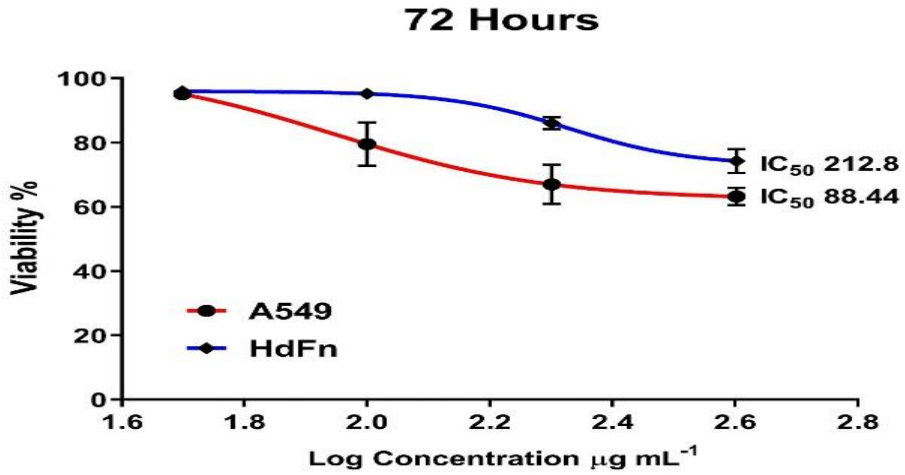

Figure 21. Cytotoxicity effect of ligand on A549 cells after 72hours of incubation at 37ºC (Log for the original concentration).

4. Conclusion

This study synthesized a new ligand by reacting the trimethoprim amide derivative with boric acid in a 1:1 mole ratio. The ligand's metal complexes were synthesized with Co(II), Ni(II), and Pt (IV) in a 2:1 (L:M) mole ratio. All synthesized compounds were characterized and confirmed the suggested structures using spectral and physicochemical methods. The results revealed the octahedral geometry of Co (II), Ni (II), and Pt (IV) complexes, which have nonelectrolyte character. The biological results showed that all the synthesized compounds possessed excellent antimicrobial activity against *Pseudomonas aeruginosa, Staph,* and *Candida albicans*. The results of the anticancer study showed that trimethoprim and the ligand have cytotoxic effects on A549 cells.

Acknowledgment

The authors thank the Department of Chemistry, College of Science, University of Baghdad for research approval.

Conflict of Interest

The authors declare that they have no conflicts of interest.

Funding

No founding.

Ethical Clearance

This work has been approved by the Scientific Committee at the University of Baghdad/ College of Science/ Department of Chemistry.

References

1. Falagas ME, Vardakas KZ, Roussos NS. Trimethoprim/sulfamethoxazole for Acinetobacter spp.: A review of current microbiological and clinical evidence. Int J Antimicrob Agents. 2015; 46(3):231–241. https://doi.org/10.1016/j.ijantimicag.2015.04.002
2. Maddileti D, Swapna B, Nangia A. Tetramorphs of the antibiotic drug trimethoprim: Characterization and stability. Crystal Growth & Design. 2015; 15(4):1745–1756. https://doi.org/10.1021/cg501772t
3. Singh AK, Kumar S, Vinayak M. Recent development in antihyperalgesic effect of phytochemicals: anti-inflammatory and neuro-modulatory actions. IR. 2018; 67(8):633–654. https://doi.org/10.1007/s00011-018-1156-5
4. Singh, S, Kumar, M, Potential therapeutic applications of trimethoprim-boric acid: A review. IJPS. 2019; 81(2):197–202. https://doi.org/10.1002/j.1875-9114.1981.tb03548.x
5. Api AM, Belsito D, Biserta S, Botelho D, Bruze M, Burton GA, Buschmann J, Cancellieri MA, Dagli ML, Date M, Dekant W, Deodhar C, Fryer AD, Gadhia S, Jones L, Joshi K, Kumar M, Lapczynski A, Lavelle M, Lee I, Liebler DC, Moustakas H, Na M, Penning TM, Ritacco G, Romine J, Sadekar N, Schultz TW, Selechnik D, Siddiqi F, Sipes IG, Sullivan G, Thakkar Y, Tokura Y. RIFM fragrance ingredient safety assessment, ethyl lactate, CAS registry number 97-64-3. FCT. 2020; 146(1):111741. https://doi.org/10.1016/j.fct.2020.111741

6. Ding R, Chen Y, Wang Q, Wu Z, Zhang X, Li B, Lin L. Recent advances in quantum dots-based biosensors for antibiotics detection. J Pharm Anal. 2022; 12(3):355-364. https://doi.org/10.1016/j.jpha.2021.08.002
7. Frei A, Zuegg J, Elliott AG, Baker M, Braese S, Brown C, Chen F, Dowson CG, Dujardin G, Jung N, King AP, Mansour AM, Massi JM, Moat KJ, Mohamed HA, Renfrew AK, Rutledge PJ, Sadler PJ, Todd MH, Willans CE, Wilson JJ, Cooper MA, and Mark Blaskovich AT. Metal complexes as a promising source for new antibiotics. Chem Sci. 2020; 11(10):2627–2639. https://doi.org/10.1039/c9sc06460e
8. Al-Adilee KJ, Abedalrazaq KA, Al-Hamdiny ZM. Synthesis and spectroscopic properties of some transition metal complexes with new azo-dyes derived from thiazole and imidazole. Asian J Chem. 2013; 25(18):10475–10481. https://doi.org/10.14233/ajchem.2013.15735
9. Farrell N. Metal complexes as drugs and chemotherapeutic agents. In: Elsevier eBooks. 2003. p. 809–840. https://doi.org/10.1016/b0-08-043748-6/09021-6
10. Desiatkina O, Johns SK, Anghel N, Boubaker G, Hemphill A, Furrer J, Paunescu, E. Synthesis and antiparasitic activity of new conjugates—organic drugs tethered to trithiolato-bridged dinuclear ruthenium (II)–arene complexes. Inorganics. 2021; 9(8):59. https://doi.org/10.3390/inorganics9080059
11. Majeed AA, Khaleel AMN. Evaluation the anticancer and biological activity by new amide compound of trimethoprim with some of its complexes. CJES. 2024; 22(1):9-22. https://doi.org/10.22124/cjes.2023.7323
12. Altahan MA, Beckett MA, Coles SJ, Horton PN, Jones CL. Synthesis and characterization of a tertiary amine: boric acid (1:1) co-crystal and a neutral zwitterionic diamine pentaboron adduct. Inorganica Chimica Acta. 2022; 539:120998. https://doi.org/10.1016/j.ica.2022.120998
13. Arkhipenko S, Sabatini MT, Batsanov AS, Karaluka V, Sheppard TD, Rzepa HS, Whiting A. Mechanistic insights into boron-catalysed direct amidation reactions. Chem Sci. 2018; 9(4):1058–1072. https://doi.org/10.1039/c7sc03595k
14. Chiu CH, Chen CT, Cheng MH, Pao LH, Wang C, Wan GH. Use of urinary hippuric acid and o-/p-/m-methyl hippuric acid to evaluate surgical smoke exposure in operating room healthcare personnel. Ecotoxicol Environ Saf. 2021; 217:112231. https://doi.org/10.1016/j.ecoenv.2021.112231
15. Shihab HM, Khaleel AMN. Synthesis of new homogeneous amino acids compound with boron and some of its metal complexes. Chem Methodol. 2023;7(2):137-155. https://doi:10.22034/chemm.2023.363773.1613
16. Abdul-Ghani AJ, Khaleel AM. Synthesis and characterizations of amide and Schiff base derived from n-substituted isatins and their complexes with some metal ions. JCP. 2009: 1458-1471. https://doi.org/10.1155/2009/413175
17. Abdul-Ghani AJ, Khaleel AMN. Synthesis and characterization of new Schiff bases derived from n (1)-substituted isatin with dithiooxamide and their Co(II), Ni(II), Cu(II), Pd(II), and Pt(IV) complexes. Bioinorganic Chemistry and Applications. 2009; 413175:1-12. https://doi.org/10.1155/2009/413175
18. Khaleel AMN, Jaafar MI. Synthesis and characterization of boron and 2-aminophenol schiff base ligands with their Cu(II) and Pt(IV) complexes and evaluation as antimicrobial agents. Orient J Chem. 2017; 33(5):2394–2404. https://doi.org/10.13005/ojc/330532
19. Drevenšek P, Košmrlj J, Giester G, Skauge T, Sletten E, Sepčić K, Turel I. X-Ray crystallographic, NMR and antimicrobial activity studies of magnesium complexes of fluoroquinolones– racemic

ofloxacin and its S-form, levofloxacin. Journal of Inorganic Biochemistry. 2006; 100(11):1755–1763. https://doi.org/10.1016/j.jinorgbio.2006.06.011

20. Siskos M, Choudhary M, Gerothanassis I. Hydrogen atomic positions of O–H···O hydrogen bonds in solution and in the solid state: The synergy of quantum chemical calculations with ^{1}H-NMR chemical shifts and x-ray diffraction methods. Molecules. 2017; 22(3):415. https://doi.org/10.3390/molecules22030415
21. Abbas AK, Kadhim RS. Synthesis, spectroscopic, thermal and antibacterial assay for azothiobutric acidlig and Co (II), Ni (II) and Cu (II) complexes. Annals of R.S.C.B. 2021; 25(6):5059-5073. http://annalsofrscb.ro/index.php/journal/article/view/6435
22. Al-adely KJ, Dakhil HK, Karam FF. Preparation and spectral characterization of new azo imidazole ligand 2-[1-(2, 4-dichoro phenyl) azo]-α-amino-1H-imidazole-4-propionic acid and its complexes with Co (п), Ni (п), Cu (п), Pd (II) and Ag (I) ions. Al-Qadisiyah Journal of Pure Science. 2017;16(2):50-64.
23. Al-Jebouri GS, Noorikhaleel AM. Synthesis of new boron compounds with amoxicillin and some of its metal complexes with use them in antibacterial, assessment of hepatoprotictive and kidneyactivity, anticancer and antioxidant applications. AJPS. 2019; 12(3):1-9. http://dx.doi.org/10.22159/ajpcr.2019.v12i3.30912
24. Khaleel AM. Synthesis and characterization of trihydro mono and dihydrobis (indole-3-acetic acid) borate ligands and some of their metal complexes. IJS. 2015; 56(4A):2762-2772.
25. Abdul-ghani AJ, Khaleel AM. Study of thermal stability of tetraphenanthroporphyrazine and somemetal complexes by thermogravimetric analysis. IJS. 2015; *56*(1B):316-328. https://ijs.uobaghdad.edu.iq/index.php/eijs/article/view/10439
26. Ali DN, Khaleel AM. Synthesis of new Schiff base of ciprofloxacin derivative with its Cu (ii), Pt (iv) complexes and evaluation of antibacterial activity. Biochem Cell Arch. 2020; 20(1):2441-2448. https://doi:10.35124/bca.2020.20.1.2441
27. Gray JR. Conductivity analyzers and their application. In: Down, R.D. and Lehr, J.H., Eds., Environmental Instrumentation and Analysis Handbook, Wiley, New York, 2004: 491-510. https://doi.org/10.1002/0471473332.ch23
28. Abbas NF, Abbas AK. Novel complexes of thiobarbituric acid–azo dye: structural, spectroscopic, biological activity and dying. Biochem Cell Arch. 2020; 20(1):2419-2433. https// doi:10.35124/bca.2020.20.1.2419
29. Jassim SA, Khaleel AM. Characterization and synthesis of new Schiff base compound from levofloxacin and L-cysteine with its Cu (II) and Pt (IV) complexes and estimation antibacterial and antifungal activities. Biochem Cell Arch. 2021; 21(1):2187-2195. https://connectjournals.com/03896.2021.21.2187
30. Ali I, Wani WA, Saleem K. Empirical formulae to molecular structures of metal complexes by molar conductance. Synthesis and Reactivity in Inorganic, Metal-Organic, and Nano-Metal Chemistry. 2013; 43(9):1162-1170. https://doi.org/10.1080/15533174.2012.756898